CSIRO PUBLISHING

International Journal of Wildland Fire **2020**, *29*, 104–119
https://doi.org/10.1071/WF19039

Current and future patterns of forest fire occurrence in China

Zhiwei Wu[A,B,C,J], *Hong S. He*[D,E], *Robert E. Keane*[F], *Zhiliang Zhu*[G], *Yeqiao Wang*[H] *and Yanlong Shan*[I,J]

[A]Key Laboratory of Poyang Lake Wetland and Watershed Research, Ministry of Education, Jiangxi Normal University, Nanchang 330022, China.
[B]School of Geography and Environment, Jiangxi Normal University, Nanchang 330022, China.
[C]Jiangxi Provincial Key Laboratory of Poyang Lake Comprehensive Management and Resource Development, Jiangxi Normal University, Nanchang 330022, China.
[D]School of Natural Resources, University of Missouri–Columbia, Columbia, MO 65211-7270, USA.
[E]School of Geographic Sciences, Northeast Normal University, Changchun 130024, China.
[F]USDA Forest Service, Rocky Mountain Research Station, Missoula Fire Sciences Laboratory, Missoula, MT 59808, USA.
[G]US Geological Survey, Reston, VA 20192, USA.
[H]Department of Natural Resources Science, University of Rhode Island, Kingston, RI 02881, USA.
[I]Forestry College, Beihua University, Jilin 132013, China.
[J]Corresponding authors. Email: wuzhiwei@jxnu.edu.cn; shanyl@163.com

Abstract. Forest fire patterns are likely to be altered by climate change. We used boosted regression trees modelling and the MODIS Global Fire Atlas dataset (2003–15) to characterise relative influences of nine natural and human variables on fire patterns across five forest zones in China. The same modelling approach was used to project fire patterns for 2041–60 and 2061–80 based on two general circulation models for two representative concentration pathways scenarios. The results showed that, for the baseline period (2003–15) and across the five forest zones, climate variables explained 37.4–43.5% of the variability in fire occurrence and human activities were responsible for explaining an additional 27.0–36.5% of variability. The fire frequency was highest in the subtropical evergreen broadleaf forests zone in southern China, and lowest in the warm temperate deciduous broadleaved mixed-forests zone in northern China. Projection results showed an increasing trend in fire occurrence probability ranging from 43.3 to 99.9% and 41.4 to 99.3% across forest zones under the two climate models and two representative concentration pathways scenarios relative to the current climate (2003–15). Increased fire occurrence is projected to shift from southern to central-northern China for both 2041–60 and 2061–80.

Additional keywords: boosted regression trees, fire probability, MODIS, relative importance.

Received 23 March 2019, accepted 27 October 2019, published online 26 November 2019

Introduction

Forest fire is a frequent disturbance that burned ~67 M ha of forests annually around the world from 2003 through 2012 (van Lierop *et al.* 2015). The effects of forest fires include short- and long-term changes in structure and function of forest ecosystems (Bond-Lamberty *et al.* 2007; Liu and Yang 2014). Fire frequency and burned area have substantially increased with prolonged growing seasons under a warming climate (Pitman *et al.* 2007; Malevsky-Malevich *et al.* 2008; Flannigan *et al.* 2009). Increases in fire frequency and burned area will pose great challenges to forests and humans (Nitschke and Innes 2008; Carvalho *et al.* 2010). For example, the Canadian wildfires from 9 to 12 June 2015 produced extensive areas of forest loss and spread of smoke across most of North America (Dreessen *et al.* 2016).

Forest fires also occur frequently in China (Adams and Shen 2015). According to Chang *et al.* (2015), there were an annual number of 8182 fires between 1987 and 2007, with an average burned area of 398 197 ha per year. Historical changes in fire frequency and burned area in regions of China are highly influenced by climate variability (Zhao *et al.* 2009; Wang *et al.* 2010; Shirazi *et al.* 2017). China's climate ranges from tropical to arctic and from wet to extremely dry, with corresponding forest ecosystems from subtropical to boreal ecotones (Piao *et al.* 2004) and resultant diverse fire regimes (Chen *et al.* 2017). Smaller fires occur most frequently in the humid and hot

subtropical evergreen broadleaf forests of southern China (Tian *et al.* 2013). In contrast, larger fires are found in the temperate-to-cool deciduous conifer forests (e.g. *Larix*) of north-eastern China and usually account for the majority of area burned in the country (Chang *et al.* 2015). The RCPs (Representative Concentration Pathways) climate scenarios released by Intergovernmental Panel on Climate Change (IPCC) show a trend of increasing temperature across China between 2011 and 2100 by 0.06°C for RCP 2.6 and 0.63°C for RCP 8.5 per decade on average from 11 General Circulation Models (GCMs) (Xu and Xu 2012). Given the projected warming trend, changes in fire frequency are therefore anticipated throughout the country.

Research into the effects of climate change on fire dynamics in China has mostly been focused on specific regions or provinces (Yang *et al.* 2012; Li *et al.* 2017). However, future effects of climate change on forest fires are projected to be highly uncertain and regionally variable (Liu *et al.* 2013). Therefore, national assessments of fire patterns and future climate must consider and summarise regional patterns and variabilities to understand broad-scale spatial patterns of fire occurrence, which may help policy makers design strategies in response to climate change.

Several studies have suggested the use of fire occurrence probability as a metric for characterising fire occurrence (Preisler *et al.* 2004; Catry *et al.* 2009; Chang *et al.* 2013; Guo *et al.* 2016). Fire probability, ranging from 0 to 1.0, is commonly defined as the probability for fires to occur in a given area (e.g. 1-km pixels) and over a defined time period (e.g. 2003–15) considering the effects of climatic and other environmental factors. In the present study, we applied the boosted regression trees (BRT hereafter) approach to model spatial patterns of fire probability under current and future climate scenarios (Liu and Wimberly 2015, 2016). The BRT modelling approach is flexible and does not rely on *a priori* assumptions of the shape of the response–predictor relationship; such an assumption is difficult for traditional linear regression models to reveal (Elith *et al.* 2008; Parisien and Moritz 2009).

In the present study, the term fire occurrence is defined as the probability of fire ignition at any location (1-km pixels) in forested lands within current (2003–15) and future (2041–60 and 2061–80) time periods. Our overall objective was to explore national-scale spatial and temporal patterns of fire occurrence under current and future climate change across China. We addressed the following specific issues: (1) how do current fire patterns vary spatially and temporally over China? (2) What are main drivers exerting the most important influence on variability in fire patterns? (3) How would China's forest fires likely respond to various scenarios of future climate?

Materials and methods

Forest zones and fire seasons

China can be generally divided into five large forest zones: (1) a cold temperate deciduous coniferous forest zone (boreal forests in the Great Xing'an Mountains of north-eastern China, with a low fire frequency but a high average burned area); (2) a temperate deciduous mixed broadleaf–conifer forest zone; (3) a warm temperate deciduous broadleaf–mixed forest zone (low forest coverage and low forest fire frequency); (4) a subtropical evergreen broadleaf forest zone (with a high forest coverage, high fire frequency but low average burned area); (5) a tropical rainforest zone (high forest coverage but low fire frequency) (Guo *et al.* 2017) (Fig. 1).

Fire seasons in China vary by geographical region and forest zone. Generally, north-eastern China (i.e. cold temperate deciduous needle-leaf forest zone and temperate deciduous mixed broadleaf and needle-leaf forest zone) has a bimodal fire season that spans March to June in spring and September to November in autumn. Fire seasons span October to May in northern China (i.e. warm temperate deciduous broadleaved mixed forests zone). There is a long fire season from November to the end of May in the southern part of China (i.e. subtropical evergreen broadleaf forest zone and tropical rainforest zone).

Data sources and data management

Fire occurrence (ignition) data

We downloaded the Global Fire Atlas dataset for January 2003–December 2015 from the FTP server ftp://fusionftp.gsfc.nasa.gov/fire_atlas/ (accessed 30 December 2018). The fire atlas was produced with support from NASA's Carbon Monitoring System program. The Global Fire Atlas was developed from the Moderate Resolution Imaging Spectroradiometer (MODIS) Collection 6 MCD64A1 burned area product (Giglio *et al.* 2018; Andela *et al.* 2019). In this dataset, clusters of burned area were subdivided into individual fires based on the spatial structure of estimated burn dates in the MCD64A1 burned area product. For each individual fire, the fire dataset contains information on the geographic location (latitude and longitude coordinates) of fire ignition (point), perimeter (polygon) and other information (fire size, duration, daily expansion, fire line length, speed and direction of spread). The MODIS-based fire data here are from a mixture of surface and crown fires. The methodology and validation of the dataset are presented in Andela *et al.* (2019), while details on the 500-m-resolution burned area product (MCD64A1 collection 6) are described in Giglio *et al.* (2018). We identified 25 729 forest fires (ignitions) between 2003 and 2015 across China with the MODIS-based Global Fire Atlas dataset, which was less than the number of forest fires recorded in the government's fire statistics dataset (103 711). The mean fire size and total burned area derived from the MODIS-based Global Fire Atlas dataset were 79.1 and 15.5% higher than those derived from the Chinese government's fire statistics dataset respectively, but the spatial distributions of forest fires from these two datasets were generally similar (Supplementary material).

The five forest zones covered 97.3% of total forest fires in China. The other 2.7% were sparsely distributed in non-forest dominated regions such as temperate steppes and deserts zones in north-western China. Specifically, the subtropical evergreen broadleaf forest zone in southern China had the highest number of fires (69.8% of the national total), followed by the tropical rainforest zone in southernmost China (15.3%), temperate deciduous mixed broadleaf and needle-leaf forest zone in central parts of north-eastern China (6.3%), then cold temperate deciduous needle-leaf forest zone north-eastern China (5.5%), and the warm temperate deciduous broadleaved mixed forest zone in central-northern China had a low fire occurrence (0.5%).

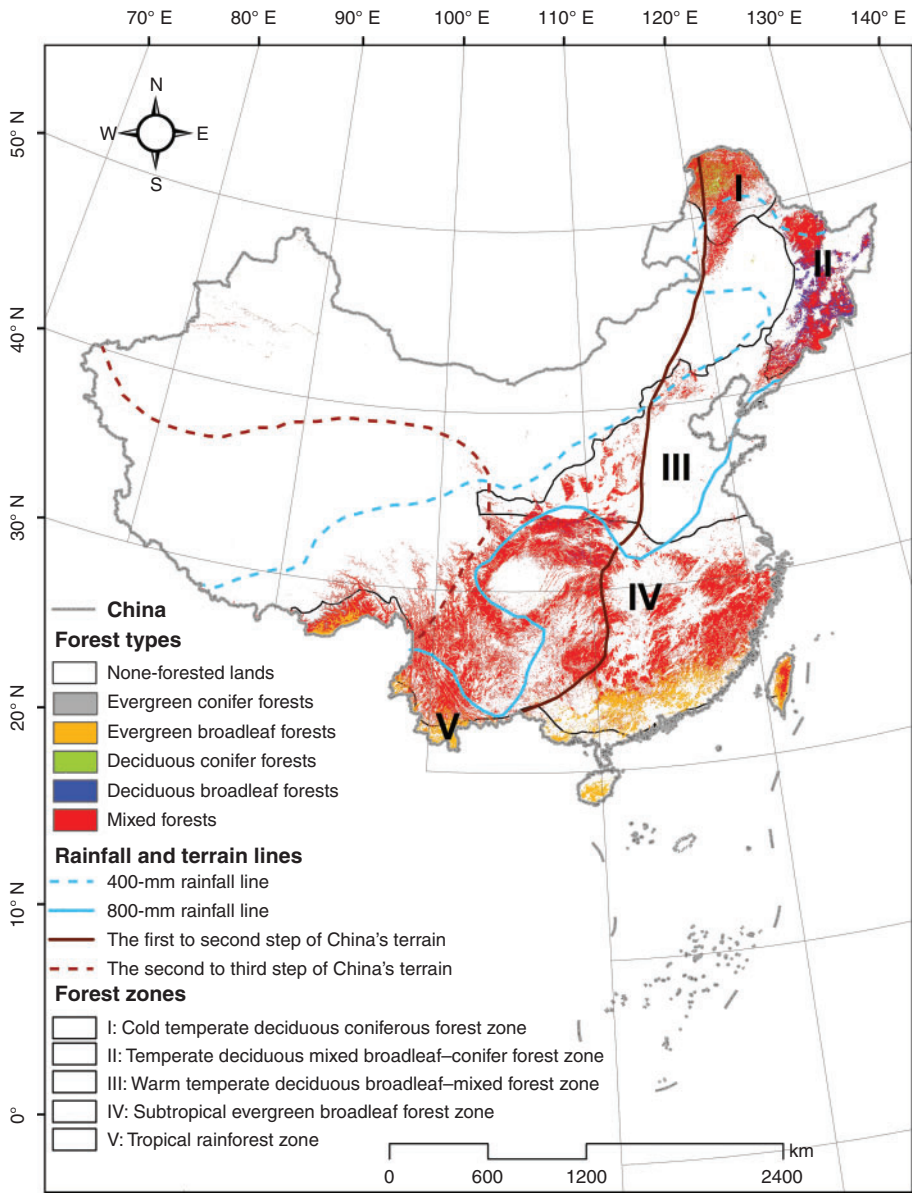

Fig. 1. Map of spatial location of China overlaid with forest types and zones, and rainfall and terrain lines.

Forest type data

Data of forest types were from the NASA MODIS Global Land Cover product (MCD12Q1) for the year 2003 at 500-m spatial resolution (https://modis.gsfc.nasa.gov/, accessed 18 January 2019). The forest types included evergreen conifer forests, evergreen broadleaf forests, deciduous conifer forests, deciduous broadleaf forests and mixed forests (Fig. 1). The overall accuracy of the MCD12Q1 product was 50.9–70.2% over China (Yang *et al.* 2017). Details about the accuracy of the MCD12Q1 product are in the Supplementary material.

Vegetation productivity (NDVI) data

The Normalized Difference Vegetation Index (NDVI) is an indicator of vegetation productivity (Hawbaker *et al.* 2013; Argañaraz *et al.* 2015). We therefore used the NDVI to represent spatial variability in vegetation productivity for the period January to December 2003–15. We derived the monthly NDVI data from the NASA MODIS Global MOD13A3 product at 1-km spatial resolution (https://modis.gsfc.nasa.gov/). We calculated the average of 13-year monthly spring (March–May), autumn (September–November) and annual mean (January–December) NDVI for the study period 2003–15.

Topography data

Elevation (m), slope (°) and aspect (Hawbaker *et al.* 2013) and a terrain-related index (e.g. topographic roughness index) (Stambaugh and Guyette 2008) have been identified as the major topographic variables related to fire occurrence. Given that slope and aspect are more properly expressed at scales less than 1 km and elevation may highly correlate with temperature

and precipitation (Parks *et al.* 2011), we therefore used a topographic roughness index to explain spatial patterns of forest fire occurrence (Stambaugh and Guyette 2008). We derived a 30-m spatial resolution grid of digital elevation model (DEM) data from the China Geospatial Data Cloud Platform (http://www.gscloud.cn/, accessed 16 June 2019). We created a surface of topographic roughness index with the DEM data based on the 'tri' function in the 'spatiaEco' package (Evans 2018) of *R* software (R Core Team 2017).

Infrastructure and population density (human-activity related data)

Anthropogenic factors such as roads, settlements and population density influence fire occurrence by increasing human-initiated ignition probability (Liu *et al.* 2012). We obtained a Global Roads Open Access Dataset (gROADSv1) covering the period 1980–2010 from the Center for International Earth Science Information Network of the Earth Institute at Columbia University (http://sedac.ciesin.columbia.edu, accessed 5 November 2018). We derived settlement points and population density data in the year 2000 from the Global Rural–Urban Mapping Project (GRUMPv1) (http://sedac.ciesin.columbia.edu). Surfaces of distance to nearest roads or settlements were created by calculating the Euclidean distance from each pixel to the nearest road or settlement with 1-km spatial resolution.

Climate data

Annual and seasonal temperature (°C) and precipitation (mm) are variables used to represent climate conditions while addressing fire characteristics (Zumbrunnen *et al.* 2009; Chang *et al.* 2015). We acquired temperature and precipitation data (January 2003–December 2015) with 0.1° × 0.1° spatial and 3-hourly temporal resolutions from the China Meteorological Forcing Dataset (http//westdc.westgis.ac.cn). The national climate dataset was derived from integration of data from 740 Chinese meteorological stations (Chen *et al.* 2011), and has been used in ecological research in various regions and ecosystems in China (Huang *et al.* 2016; Dai *et al.* 2018). We calculated the average of the 13-year spring (March–May), summer (June–August), autumn (September–November), winter (December–February) and annual mean (January–December) temperature and precipitation for the study period of 2003–15.

Future GCM data of annual temperature and precipitation with 5-min resolution of longitude and latitude degrees were obtained from the WorldClim version 1.4 (http://worldclim.org/) (Hijmans *et al.* 2005). Based on the GCMs outputs in the WorldClim-Global climate dataset, we selected GFDL-CM3 (Geophysical Fluid Dynamics Laboratory) and GISS-E2-R (NASA Goddard Institute for Space Studies) to capture uncertainties regarding future climate change. The GFDL-CM3 is relatively hot and wet, whereas GISS-E2-R projects a relatively cold and dry future. For each of the two GCMs, we used two scenarios of greenhouse gas concentrations (RCP 2.6 and 8.5) and two periods: 2050 (average for 2041–60) and 2070 (average for 2061–80). The RCP 2.6 scenario assumes that annual global greenhouse gas concentration peaks between 2010 and 2020, and declines substantially thereafter. In the RCP 8.5, concentrations would continue to rise throughout the 21st century (Meinshausen *et al.* 2011). The future climate projected by the two GCMs in WorldClim version 1.4 had been calibrated using historical climate layers (1960–90). Details on the historical climate layers can be found in Hijmans *et al.* (2005). We compared historical mean annual temperature and precipitation from WorldClim (1960–90) with observations from 613 benchmark weather stations (1960–90) across China (http://data.cma.cn/site/index.html). Results showed that historical annual temperature and precipitation values from these two datasets were close (Supplementary material), indicating validity of using the GCM data for future climate in the present study.

Mean annual temperature in China would increase significantly under both the RCPs, ranging from 2.2° to 8.5°C across all five forest zones by 2041–60 and 2061–80 (Fig. 2). Most of the forest zones had increasing trends projected in mean annual precipitation under GFDL-CM3 that ranged from 5.8 to 219.4 mm, but only the RCP 8.5 scenario of 2041–60 projected a decreasing trend in forest zones III (−24.5 mm) and IV (−57.7 mm). For the GISS-E2-R, forest zones II and IV had a decreasing trend in mean annual precipitation change ranging from −8.3 to −48.3 mm projected. Other forest zones generally had an increasing trend in mean annual precipitation change ranging from 0.17 to 64.8 mm projected, but only the RCP 8.5 scenario of 2041–60 projected a decreasing trend in forest zones I (−8.4 mm) and III (−24.5 mm), and RCP 2.6 in zone I (−57.7 mm) (Fig. 3).

Analysis

We modelled patterns of forest fires with 1-km spatial resolution. We resampled all the climate, vegetation, topography and human activity layers to 1-km spatial resolution in the *ArcGIS* environment. We resampled continuous variables (layers) using the bilinear interpolation method and categorical variables using the nearest-neighbour method. The focus of this study was to explore spatial patterns of forest fires. Therefore, the non-forested areas were excluded from data analyses based on the MCD12Q1 product.

We created a fire-point dataset based on the latitude and longitude coordinates of fire ignition location from the Global Fire Atlas dataset. We overlaid the fire-point dataset with the pixels of the 1-km gridded forest-type data (extracted from the MODIS MCD12Q1 product). The pixels of forest-type data with one or more fire occurrences (ignitions) observed were coded as '1', representing fire occurred, and non-fire pixels were coded as '0'. The '0,1' dataset was subsequently used as the response (y) variable in BRT models. We randomly sampled the '0/1'-coded pixels for each forest zone to construct and validate BRT models. The number of sampling pixels for each forest zone was determined using the equation according to Peduzzi *et al.* (1996):

$$N = \frac{10 \times k}{p}$$

where N is the number of sampling pixels; k is the number of explanatory variables; p is the proportion of fire pixels in each forest zone.

There were 8713, 11 675, 54 609, 5283 and 3191 sampling pixels for the five forest zones I–V. We randomly separated the

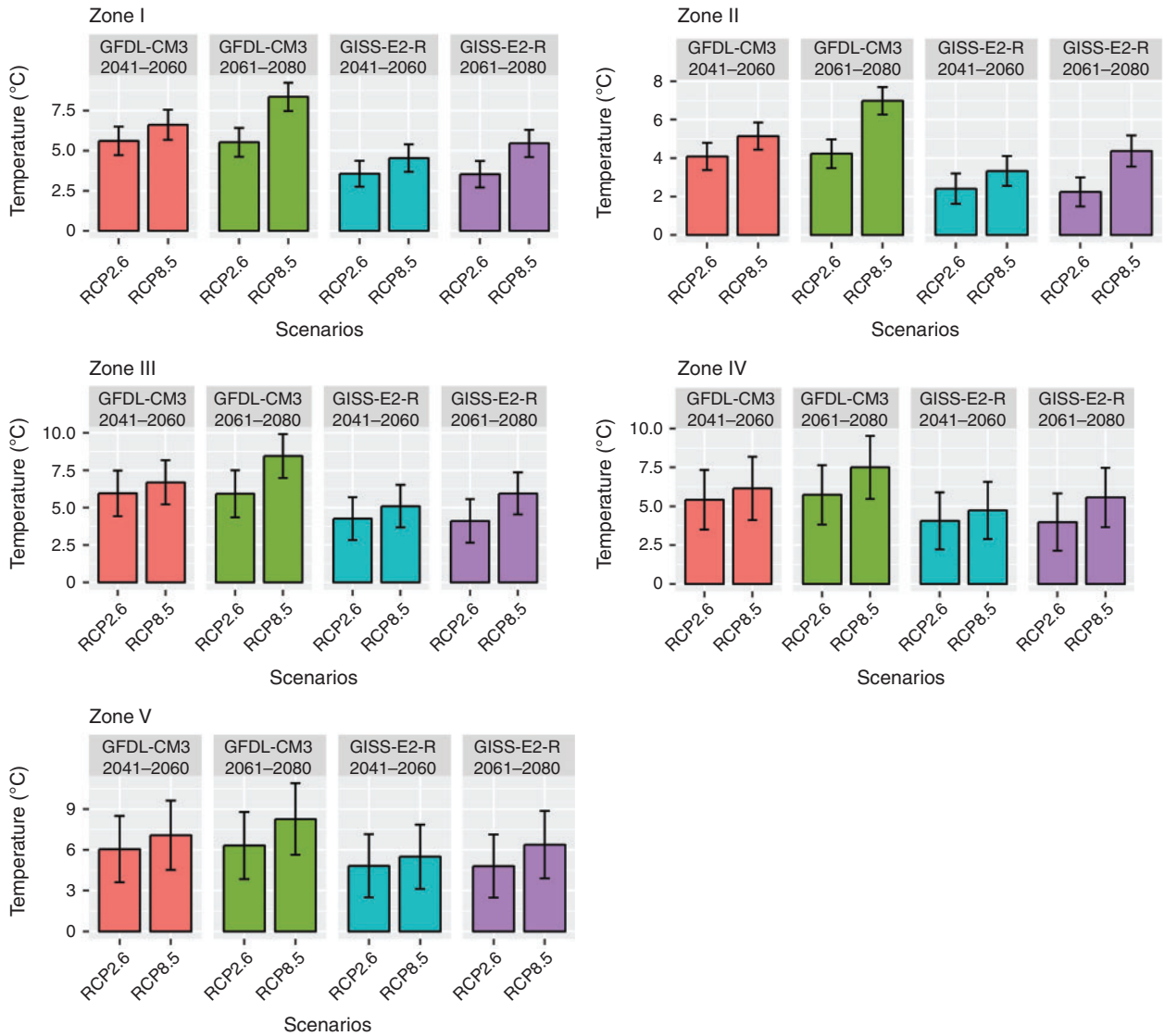

Fig. 2. Changes (mean ± s.d.) in annual temperature (°C) (future minus current) for future RCPs (Representative Concentration Pathways) scenarios (RCP 2.6 and RCP 8.5) under two Global Circulation Models (GFDL-CM3 and GISS-E2-R) in years 2041–60 and 2061–80 by forest zone. Forest zones refer to Fig. 1.

sample-pixel dataset into a training dataset (70%) and a validation dataset (30%) for each forest zone. This subsampling procedure was performed five times for each forest zone, resulting in five random subsamples of datasets. We extracted values of all 22 explanatory variables (Table 1) for these sample pixels for the five forest zones. We used the training dataset to construct BRT models and the validation dataset to evaluate the performance of models for each forest zone.

High correlation between explanatory variables may make variable redundant in a model. It is also important to reduce collinearity to strengthen the interpretation of BRT model outputs (e.g. the relative importance of variables). We used the Generalised Variance Inflation Factor (GVIF) approach to test for possible multicollinearity among the 22 explanatory variables (Fox and Monette 1992). We used the rule of thumb that when the GVIF index >5, then the collinearity of given explanatory variables would be problematic and they should be removed in the iterative process. As the result, we only included nine explanatory variables in subsequent fire occurrence model fitting and data analyses (Table 1).

Converting fire occurrence to fire probability (BRT model construction)

We applied the boosted logistic regression trees (BRT) approach to model spatial patterns of fire probability for the entire 13 years (2003–15) based on the training data from the Global Fire Atlas dataset. The BRT model is a form of logistic regression that models the probability of a fire occurring, $y = 1$, at a location with explanatory variables (covariates) X, $P(y = 1|X)$. The fire probability is modelled via a logit function: logit $P(y = 1|X) = f(X)$. To minimise predictive error, we tested several combinations of key fitting parameters of the BRT

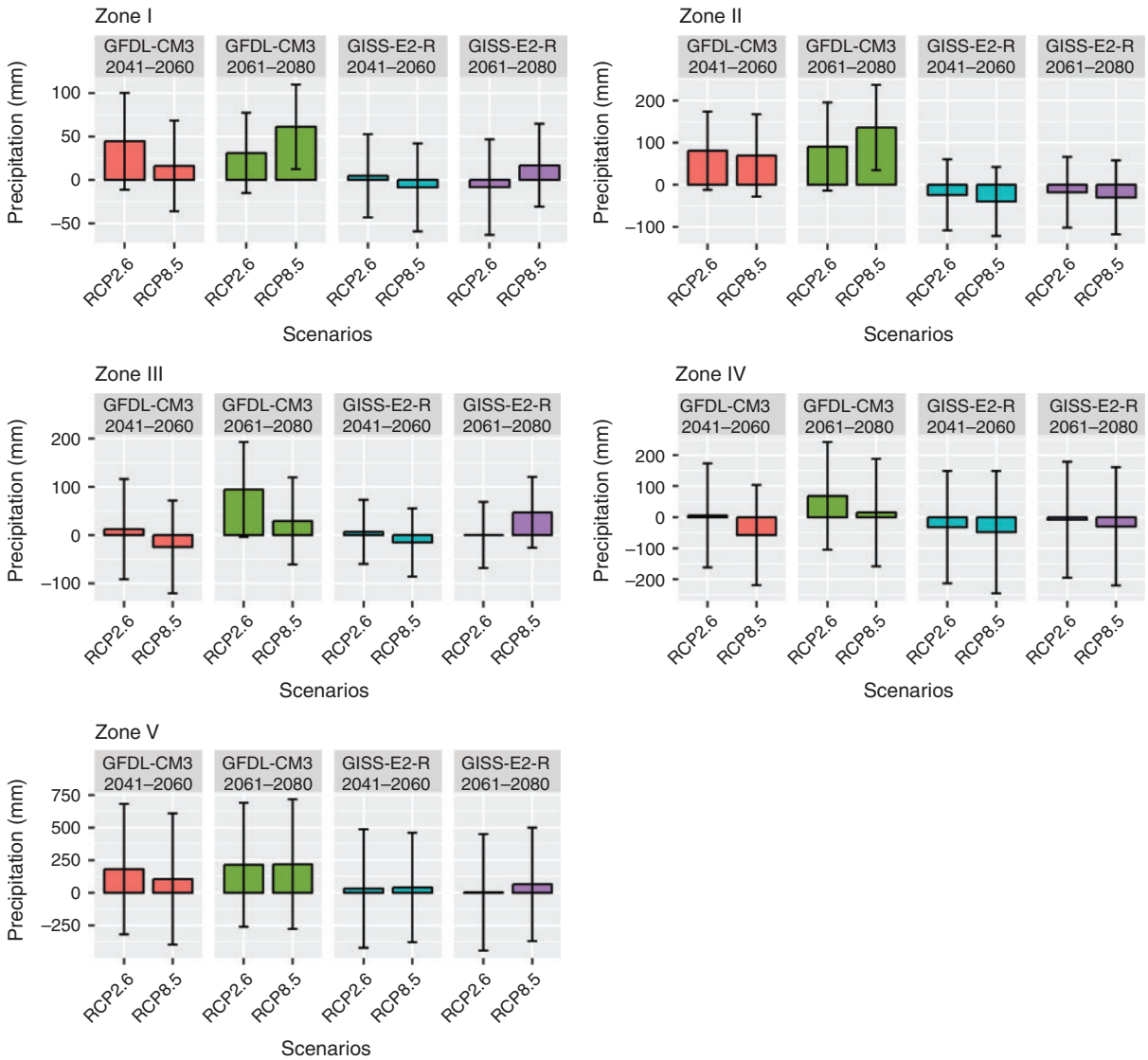

Fig. 3. Changes (mean ± s.d.) in annual precipitation (mm) (future minus current) for future RCPs (Representative Concentration Pathways) scenarios (RCP 2.6 and RCP 8.5) under two Global Circulation Models (GFDL-CM3 and GISS-E2-R) in years 2041–60 and 2061–80 by forest zone. Forest zones refer to Fig. 1.

model (learning rate, tree complexity and number of trees) as recommended by Elith *et al.* (2008) (Table 2). We ran the BRT models five times using the randomly sampled training dataset (70%) for each forest zone. We used the 'gbm' package (Greenwell *et al.* 2018) in *R* (R Core Team 2017) to construct BRT models referencing the *R* scripts developed by Elith *et al.* (2008).

We evaluated the performance of the BRT models using the area under curve (AUC) of a receiver operating characteristic curve (ROC) plot with the randomly sampled validation dataset (30%) for each forest zone. The AUC was used to measure the probability of correctly classifying a random pair of fire and non-fire observations. AUC values varied from 0.5 (random discrimination) to 1.0 (perfect discrimination), and values above 0.8 indicated excellent performance of a model in discrimination (Vilar del Hoyo *et al.* 2011; Guo *et al.* 2016). We calculated the AUC values with the 'ROCR' package (Sing *et al.* 2005) in *R* (R Core Team 2017).

Quantifying relative importance of explanatory variables

We used the BRT models to quantify the relative importance of explanatory variables on fire probability for each forest zone. The BRT model calculated the relative importance of explanatory variables using the formula developed by Friedman (2001). Calculations of a variable's relative importance in the BRT model were based on how often a variable was selected in splitting a tree (tree node), weighted by the squared improvements to the model as a result of each split, and averaged over all trees (De'ath 2007; Elith *et al.* 2008). This gave a relative

Table 1. Summary of vegetation, topography, human and climate variables used in explaining and predicting fire occurrence
GVIF (Generalised Variance Inflation Factor) was used to measure the amount of multicollinearity in the explanatory variables. This study used the rule of thumb that when GVIF > 5, then collinearity in the explanatory variable exists and is excluded in the boosted regression tree model construction. NDVI, Normalized Difference Vegetation Index.

Variable group	Variable name	Unit	GVIF value	Source and original spatial resolution
Vegetation	Forest type	Class 1–5	3.3	NASA MODIS Global MCD12Q1 Product (https://modis.gsfc.nasa.gov/), 500 m
	Mean spring NDVI (March–May)	Range: –1 to 1	3.1	NASA MODIS Global MOD13A3 Product (https://modis.gsfc.nasa.gov/), 1 km
	Autumn NDVI (September–November)	Range: −1 to 1	>5.0	
	Annual NDVI (January–December)	Range: −1 to 1	>5.0	
Topography	Topographic roughness index	Dimensionless	1.3	China Geospatial Data Cloud Platform (http://www.gscloud.cn/), 30 m
Human	Distance to nearest road	km	1.5	Center for International Earth Science Information Network (http://sedac.ciesin.columbia.edu), shape files
	Distance to nearest settlement	km	1.6	
	Population density	No. people km^{-2}	1.1	
Climate	Max. spring temperature (March–May)	°C	>5.0	China Meteorological Forcing Dataset (http//westdc.westgis.ac.cn), 0.1° × 0.1°
	Min. spring temperature (March–May)	°C	>5.0	
	Max. summer temperature (June–August)	°C	2.5	
	Min. summer temperature (June–August)	°C	>5.0	
	Max. autumn temperature (September–November)	°C	>5.0	
	Min. autumn temperature (September–November)	°C	>5.0	
	Max. winter temperature (December–February)	°C	>5.0	
	Min. winter temperature (December–February)	°C	>5.0	
	Annual temperature (January–December)	°C	>5.0	
	Mean spring precipitation (March–May)	mm	>5.0	
	Mean summer precipitation (June–August)	mm	>5.0	
	Mean autumn precipitation (September–November)	mm	2.2	
	Mean winter precipitation (December– February)	mm	2.2	
	Mean annual precipitation (January–December)	mm	>5.0	

measure of variable importance in the BRT model. The relative importance of each variable was scaled so that the sum added to 100; a higher number indicated stronger influence on fire occurrence (Elith *et al.* 2008).

Projection of future fire changes

Future fire probabilities were projected using the BRT model for 2041–60 and 2061–80 under the two GCM models and two RCP scenarios and assuming stable vegetation and other environmental and human variables. Relative changes of fire occurrence probability for each 1-km pixel between the baseline (current) and future years were calculated as:

$$\Delta P_{\text{change}} = \frac{P_{\text{future}} - P_{\text{current}}}{P_{\text{current}}} \times 100\%$$

where P_{future} and P_{current} represent fire probability for future years (2041–60 and 2061–80) and current baseline (2003–15) respectively; ΔP_{change} represents changes of fire probability between current and future climate scenarios.

Results

Model valuation

The baseline fire models (BRTs) were evaluated against the AUC statistic, and the evaluation showed satisfactory results in discriminating presence or absence of fire on a pixel basis. The AUC values ranged between 0.831, 0.887, 0.820, 0.702 and 0.761 for forest zones I, II, III, IV and V respectively (Fig. 4). As noted before, an AUC value of 0.5 represents random assignment whereas 1.0 represents perfect discrimination.

Relative importance of explanatory variables in the models

We ranked explanatory variable groups by forest zones according to their total relative contribution (relative importance) (Table 3). Specifically, according to the relative importance values (%) calculated with the BRT models for explanatory variables by forest zones, the set of climate variables ranked first in forest zones I (41.8%), II (37.1%), III (40.5%), IV (43.1%) and V (43.5%). The human variable group was another important contributor and ranked second in forest zones I (33.6%), II (32.8%), III (27.0%), IV (31.9%) and V (36.5%). Vegetation (10.4–23.9%) and topography (9.3–10.3%) variable groups generally ranked low in terms of their contributions to fire occurrence. For individual variables, we found that temperature, precipitation, population density, distance to settlement and vegetation productivity (NDVI) were commonly ranked as the most important variables, whereas variables of forest type and topographic roughness index were less important in most forest zones in China (Fig. 5).

Spatial patterns under current climate

The fire probability, as shown on the Fig 6*b*, developed using the BRT model ranged from 0.0006 to 0.7726 with a median value of 0.0118 across the entire forested land of China between 2003

Table 2. Key fitting parameters of final boosted regression tree (BRT) models for five random samples of each forest zone

Parameters were selected based on the stepwise procedure. Family specifies the distribution of the response variable in the BRT tree model (here the Bernoulli distribution for binary "0,1" fire occurrence data). The learning rate determines the contribution of each tree to the growing BRT tree models, and the tree complexity controls the maximum depth of each tree (i.e. highest level of variable interactions allowed). Number of trees specifies total number of trees to be fitted in BRT models. Forest zones refer to Fig. 1

Forest zones	Samples	Parameters			
		Family	Learning rate	Tree complexity	Number of trees
Zone I	Sample 1	Bernoulli	0.001	5	650
	Sample 2	Bernoulli	0.0025	5	1400
	Sample 3	Bernoulli	0.001	5	850
	Sample 4	Bernoulli	0.005	5	600
	Sample 5	Bernoulli	0.005	5	700
Zone II	Sample 1	Bernoulli	0.0025	5	2300
	Sample 2	Bernoulli	0.01	4	650
	Sample 3	Bernoulli	0.005	5	1150
	Sample 4	Bernoulli	0.0025	5	1200
	Sample 5	Bernoulli	0.0025	5	1400
Zone III	Sample 1	Bernoulli	0.005	5	500
	Sample 2	Bernoulli	0.0025	5	3450
	Sample 3	Bernoulli	0.005	5	1100
	Sample 4	Bernoulli	0.01	5	300
	Sample 5	Bernoulli	0.005	5	1350
Zone IV	Sample 1	Bernoulli	0.0025	4	950
	Sample 2	Bernoulli	0.001	5	800
	Sample 3	Bernoulli	0.001	5	1400
	Sample 4	Bernoulli	0.001	3	1150
	Sample 5	Bernoulli	0.001	5	950
Zone V	Sample 1	Bernoulli	0.005	4	550
	Sample 2	Bernoulli	0.0025	5	850
	Sample 3	Bernoulli	0.001	5	2300
	Sample 4	Bernoulli	0.005	4	500
	Sample 5	Bernoulli	0.001	5	2000

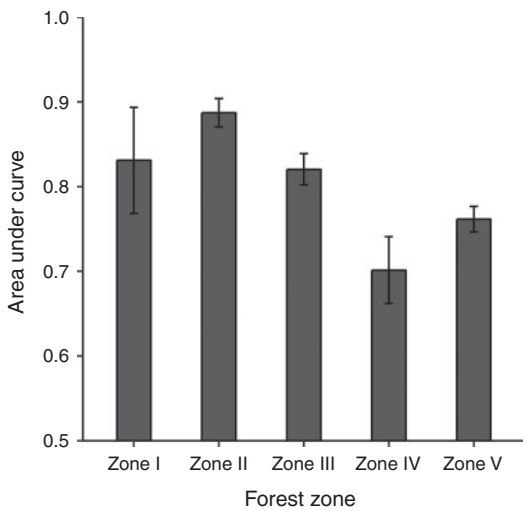

Fig. 4. Area under curve of the receiver operating characteristics curve for boosted regression tree models with the 30% validation dataset by forest zone. Forest zones refer to Fig. 1.

and 2015. These results indicate that within a 1-km pixel, there would be as low as 0.06% and as high as 77.3% chance of a fire occurring over the 13 years of study. We found considerable variability in the estimated probability of fire occurrence among and within the five forest zones. Predicted high probability was generally distributed in north-eastern and southern China. Central-northern China was identified as having lower probability of fire occurrence throughout (Fig. 6*b*). Moreover, the BRT model-predicted fire patterns generally agreed with the MODIS observed fires (Global Fire Atlas dataset) (Fig. 6*a*).

Spatial patterns under future climate

In general, future fires projected under climate change scenarios had similar distributions (fires mainly located in southern and north-eastern China) compared with the baseline, but with increased values of fire occurrence probability (Fig. 7). In the results, areas with projected high probability of fire appear to have shifted from southern to central-northern China, which was more significant under the GFDL-CM3 climate scenarios (Fig. 8).

Specifically, the percentage of pixels with an increasing trend in fire probability ranged from 43.3 to 99.9% under the GFDL-CM3 scenarios, and 41.4 to 99.3% under the GISS-E2-R scenarios compared with the current climate. Within

Table 3. Explanatory variable groups ranked according to their relative importance value (%) calculated with boosted regression tree (BRT) models for each forest zone

The relative importance value (relative influence) of explanatory variables measures the number of times variables are selected for splitting trees weighted by the squared improvement to BRT models. Group names refer to Table 1 and forest zones refer to Fig. 1

Forest zone	First		Second		Third		Fourth	
	Group name	Importance	Group name	Importance	Group name	Importance	Group name	Importance
Zone I	Climate	41.8	Human	33.6	Vegetation	14.3	Topography	10.3
Zone II	Climate	37.4	Human	32.8	Vegetation	20.5	Topography	9.3
Zone III	Climate	40.5	Human	27.0	Vegetation	23.9	Topography	8.6
Zone IV	Climate	43.1	Human	31.9	Vegetation	14.8	Topography	10.2
Zone V	Climate	43.5	Human	36.5	Vegetation	10.4	Topography	9.6

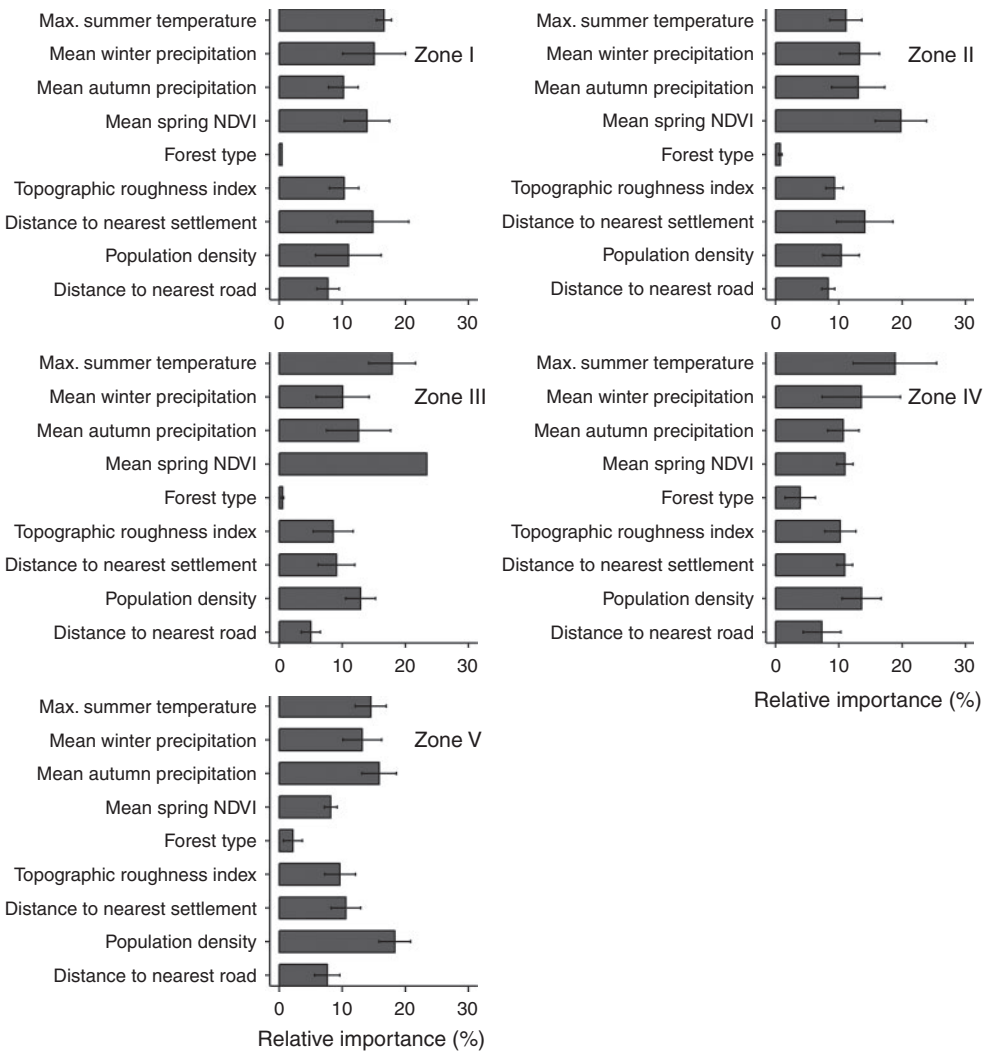

Fig. 5. Relative importance (%) (mean ± s.d.) of explanatory variables on fire occurrence probability by forest zones. Forest zones refer to Fig. 1. NVDI, Normalized Difference Vegetation Index.

GFDL-CM3, the highest fire probability increase (by 99.9%) was in zone I (RCP 8.5 in 2061–80) and lowest (by 43.3%) in zone V (RCP 2.6 in 2061–80). For GISS-E2-R, the highest increase (99.3%) was seen in forest zone I (RCP 8.5 in 2061–80) and lowest (41.4%) in zone V (RCP 2.6 in 2041–60) (Table 4).

For each RCP scenario by forest zone and GCM model, we divided the percentage of pixels with an increasing trend of fire

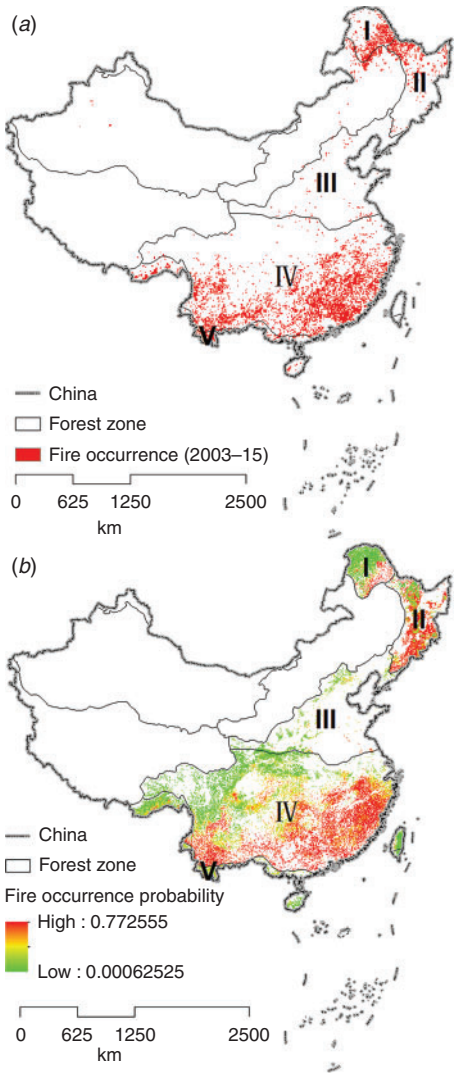

Fig. 6. Spatial distribution of (*a*) fire occurrence (2003–15), and (*b*) boosted regression tree model predicted fire occurrence probability under current climate.

occurrence probability in 2061–80 by percentage of pixels with an increasing trend of fire occurrence probability in 2041–60 (Table 4). We found that there were no remarkable differences in changes of fire probability between 2041–60 and 2061–80 for both GFDL-CM3 and GISS-E2-R scenarios. Specifically, for both the GCM models and both RCP scenarios, the percentage of pixels with an increasing trend of fire occurrence probability in 2061–80 was 0.87–1.15 times that in 2041–60 (Table 4).

Discussion

Effects of explanatory variables

Forest fires in China were not randomly distributed but showed an aggregative distribution pattern, mainly located in the south and north-east parts of China, demonstrating that fire occurrence is not a random process, but exhibits a high degree of clustering on landscapes and regionally, driven by climate (Tian *et al.* 2013; Chang *et al.* 2015). This situation has been observed in other countries such as the United States (Hawbaker *et al.* 2013) and Australia (Russell-Smith *et al.* 2007).

Spatial patterns of forest fires are a function of numerous influencing factors such as climate, topography, vegetation and human activity. Among the factors considered in this study in China, we found that climatic factors have the greatest influence on patterns of fire occurrence, which is in agreement with results from an extensive body of fire-science studies (Pitman *et al.* 2007; Flannigan *et al.* 2009; Liu *et al.* 2012), such as wildfires of United States (Hawbaker *et al.* 2013) and Australia (Russell-Smith *et al.* 2007). In the present study, it is evident that higher fire probabilities are correlated strongly with increased precipitation (rainfall), which favours vegetation growth (i.e. increasing biomass production) if there are also related high temperature (drier fuels) conditions in the region (O'Donnell *et al.* 2011; Zhang and Lim 2019). However, there are some other underlying causes that shape fire patterns in China. Previous studies have suggested that fire patterns may be associated with weather events such as thunderstorm activity that are related to precipitation and warm temperatures, and could provide a mechanism for starting fires (e.g. lighting fires). For example, Liu *et al.* (2012) suggested that areas with the greatest chance of lightning fires were distributed in the northern part of forest zone I (cold temperate deciduous coniferous forests in north-eastern China), which coincides with the highest predicted increases of annual temperature and precipitation.

We found that human activity variables (e.g. distance to nearest settlements and roads) were also important in shaping fire patterns. These findings reinforce claims that, despite the strong influence of climate, effects of human activities cannot be ignored (Syphard *et al.* 2007; Achard *et al.* 2008; Ganteaume *et al.* 2013). For example, Russell-Smith *et al.* (2007) found that most fires in Australia appears to be anthropogenic, especially in the northern wet–dry tropics and arid Australia. In the United States, human-related variables were ranked highest in explaining fire occurrence patterns in the Central Plains, the Mixedwood Plains, and the Ozark Ouachita Appalachian forests (Hawbaker *et al.* 2013). Some studies have suggested that fire occurrence was high when the distance to settlements or roads is low (Romero-Ruiz *et al.* 2010). For example, Catry *et al.* (2009) reported that ~98% of fires occurred less than 2 km from the nearest roads in Portugal. In China, for example, a large number of people reside in low-relief plains in forest zone II (the temperate deciduous mixed broadleaf–conifer forests) and have a significant influence on regional fire regimes, especially from their farming activities, as they tend to burn crop residues before planting (Zhang *et al.* 2015). Forest zone III is characterised by low forest coverage and low forest fire frequency, but these areas may burn if given a chance, particularly under higher human activity and warmer climate conditions. It is worth noting that in China, fires in areas with high population density are easier to detect and suppress in time once they occur, and consequently the burnt area is usually smaller than in areas with low population density, such as in forest zone I (cold temperate deciduous coniferous forests zone).

Under current conditions, fires were most frequent in the evergreen broadleaf forest zone (zone IV) located in the southern part of China. In this region, fires occur in coniferous forests,

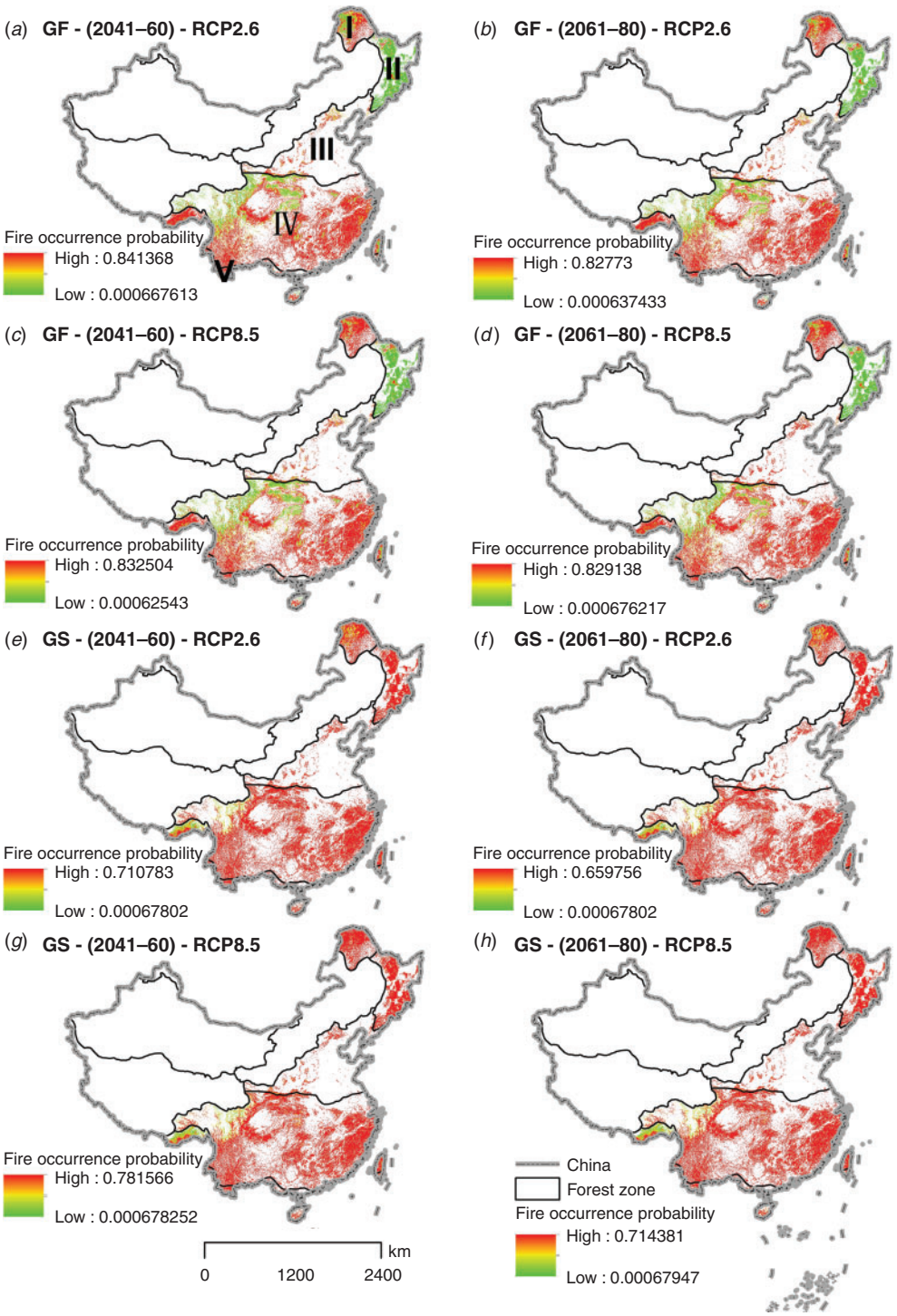

Fig. 7. Predicted fire occurrence probability by Global Circulation Models (GF: GFDL-CM3; GS: GISS-E2-R) and Representative Concentration Pathways (RCP) scenarios (RCP 2.6 and 8.5) and time periods (2041–60 and 2061–80).

such as Masson pine (*Pinus massoniana*) and Chinese fir (*Cunninghamia lanceolata*) forests (Pan *et al.* 2013). The high frequency of fires in this zone is related to the strong effects of climate and human activity. In southern China, strong and dry valley winds occur frequently in early spring each year, which thus leads to favourable conditions for fire ignitions (Chang *et al.* 2015). Moreover, road networks are well developed and population density is high in this region. Agricultural cultivation is also near settlements and roads in this region. Fire is a popular tool for agricultural activities (e.g. burning grasses), and

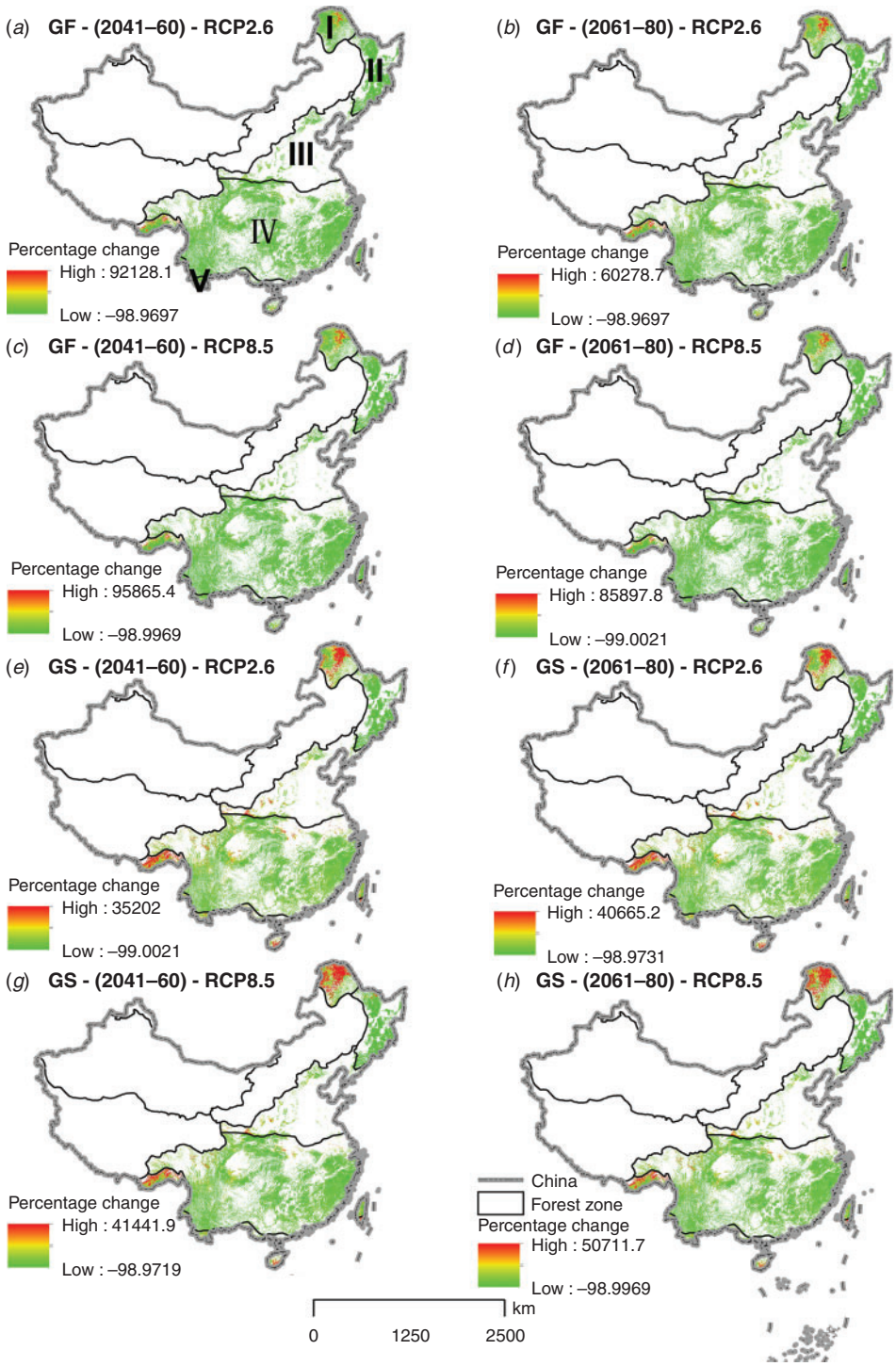

Fig. 8. Relative changes in fire occurrence probability between future Representative Concentration Pathways scenarios (RCP 2.6 and 8.5) and current climate by Global Circulation Models (GF: GFDL-CM3; GS: GISS-E2-R) and time periods (2041–60 and 2061–80).

agricultural fires have escaped and burned adjacent forests frequently in this region (Tian *et al.* 2013).

Compared with climate and human activities, forest types in China have a relatively small role in our model in explaining fire patterns across all five forest zones. With strong effects from climate and human activities, it is possible that effects by forest types are already explained in effects of climate (e.g. temperature and precipitation) and human activities. Moreover, we

Table 4. Percentage change of pixels with increased fire occurrence probability from general circulation models (GFDL-CM3 and GISS-E2-R) and RCP (Representative Concentration Pathways) scenarios (RCP2.6 and 8.5) and time periods (2041–60 and 2061–80) compared with current climate

Forest zones refers to Fig. 1

Forest zone	Time	GFDL-CM3		GISS-E2-R	
		RCP2.6	RCP8.5	RCP2.6	RCP8.5
Zone I	2041–60	99.6	99.8	78.9	94.1
	2061–80	99.8	99.9	82.5	99.3
Zone II	2041–60	95.8	97.1	94.8	95.4
	2061–80	96.2	96.7	94.3	96.6
Zone III	2041–60	96.8	96.7	89.5	91.6
	2061–80	95.1	97.0	88.1	94.6
Zone IV	2041–60	84.0	89.6	70.4	76.5
	2061–80	83.1	92.2	69.3	81.5
Zone V	2041–60	50.0	51.0	43.3	44.4
	2061–80	43.3	59.6	41.4	51.1

modelled fire occurrence patterns using forest type data at 1-km spatial resolution, which may not capture spatial variation of forest type well.

Effects of climate change on future fire patterns

The GFDL-CM3 projections are relatively warmer (higher temperature) and wetter (higher precipitation) than those of GISS-E2-R (Figs 2 and 3). Normally, wetter climate projections should lead to decreased fire activities. However, our results showed that the GFDL-CM3 scenarios projected greater increases in fire occurrence than the GISS-E2-R scenarios (Table 4). This supports the claim that an increase in temperature would greatly offset increases in precipitation at a broad scale (Boulanger *et al.* 2013), particularly in forest zone I (cold temperate coniferous forests in north parts of north-eastern China). In a forest landscape, higher temperatures can contribute to increasing transpiration and thus decreasing moisture content of live fuels, leading to an increase in the probability of fire occurrence. Moreover, previous studies have shown that warmer climates could extend vegetation growing seasons and increase plant production and dry fuel availability in late autumn, and consequently fire occurrence would increase substantially. For example, warmer climates and longer vegetation growing seasons in recent decades explain much of the large fire occurrence patterns in the western United States (Westerling *et al.* 2006; Westerling 2016).

Our results showed that some regions in China such as forest zones I (north parts of north-eastern China) and III (central-northern China) would experience significant increases in fire probability in future years compared with the current period, whereas other areas (e.g. most areas of forest zone V) would remain stable. The regional variability is generally consistent with the relative importance of the explanatory variables under baseline conditions (2003–15). For example, forest zone I (i.e. boreal forests of north-eastern China) is projected to have future higher temperatures (Fig. 3) compared with current conditions; at the same time, 78.9–99.3% of the zone is projected to have increased fire probabilities in 2041–60 and 2061–80. This is similar to recent findings in the literature such as Liu *et al.* (2012) where fire density (number of fires per 1000 km^2 per year) in the boreal forests of China is reported to increase 30–230% in 2081–2100. But we also found that the effect of climate change on fire occurrence was constrained by human activity. For example, although temperature would increase across all scenarios in both 2041–60 and 2061–80 in forest zone V (southern China), only 41.4–59.6% of pixels would show an increasing trend. In southern China, agricultural cultivation is mixed with developed lands and fire is a popular tool for agricultural activities (e.g. burning grasses on wasteland). Agricultural fire use has become a major source of forest fires. We therefore assume that the temperature effect was constrained by human activity effects, which explained 36.5% of the spatial variation of fire occurrence in forest zone V.

Limitations and uncertainties

Long-term and large-scale data are important for projecting responses of wildland fires to climate change. However, such historical data are usually unavailable or inconsistent, which may lead to limitations and uncertainties in our study. Fire occurrences were modelled together regardless of fire types (e.g. lightning-caused fires and human-caused fires) in this study. Lightning-caused fires occur more often in isolated and high-elevation areas, whereas human fires show different distribution patterns as they are most frequent at lower elevations with high population density. Therefore, the relative importance of the explanatory variables (e.g. vegetation and topographic parameters in this study) may be different if lightning-caused fires and human-caused fires were modelled separately.

We used the 13-year temperature and precipitation data to build the fire occurrence model. Short-term climate data may not capture long-term variability of the fire–climate relationship (Hawbaker *et al.* 2013), which may affect the comparability of fire occurrence under current (2003–15) and future climates (2041–60 and 2061–80). Short-term studies should be carefully examined when extrapolating the results to long-term fire–climate relationships. Furthermore, given that fires tend to occur following drought events, it would be valuable in such a study to include antecedent climate, e.g. drought conditions for half a month before fire ignition.

We assumed human activity and vegetation during 2041–60 and 2061–80 would be similar to the present (2003–15), but fire patterns could be a function of changes in vegetation composition, structure and distribution because of climate change (Mitchell *et al.* 2014; Keane *et al.* 2018). The changed vegetation structures and patterns could affect fire regimes in future (Pausas and Bradstock 2007) in different relationships, which would in turn alter the composition and structure of forests. The next step therefore would be to incorporate vegetation dynamics models to address feedback effects of vegetation to fire caused by a changing climate (Flannigan *et al.* 2005).

Conclusions

Forest fires primarily occurred in southern, south-western and north-eastern China during the years between 2003 and 2015. Climate variables had primary effects on spatial variability of

fire occurrence; human activities were secondary. The modelling results showed that, under future climate scenarios, the percentage of pixels with an increasing trend in fire probability ranged from 41.4 to 99.9%. High-fire-occurrence regions would shift from south to central-north parts of China for both 2041–60 and 2061–80. This research will aid in providing a national-scale understanding of future potential fire patterns in China and help policymakers to design fire management strategies to mitigate potential risks.

Conflicts of interest

The authors declare no conflict of interest.

Acknowledgements

This research was funded by the National Natural Science Foundation of China (grant no. 31570462) and the Scientific and Technological Research Project of Jiangxi Provincial Department of Education (grant no. GJJ160275).

References

Achard F, Eva HD, Mollicone D, Beuchle R (2008) The effect of climate anomalies and human ignition factor on wildfires in Russian boreal forests. *Philosophical Transactions of the Royal Society of London. Series B, Biological Sciences* **363**, 2329–2337. doi:10.1098/RSTB.2007.2203

Adams MA, Shen ZH (2015) Introduction to the characteristics, impacts and management of forest fire in China. *Forest Ecology and Management* **356**, 1. doi:10.1016/J.FORECO.2015.09.019

Andela N, Morton DC, Giglio L, Paugam R, Chen Y, Hantson S, van der Werf GR, Randerson JT (2019) The Global Fire Atlas of individual fire size, duration, speed and direction. *Earth System Science Data* **11**, 529–552. doi:10.5194/ESSD-11-529-2019

Argañaraz JP, Pizarro GG, Zak M, Landi MA, Bellis LM (2015) Human and biophysical drivers of fires in semiarid Chaco mountains of central Argentina. *The Science of the Total Environment* **520**, 1–12. doi:10.1016/J.SCITOTENV.2015.02.081

Bond-Lamberty B, Peckham SD, Ahl DE, Gower ST (2007) Fire as the dominant driver of central Canadian boreal forest carbon balance. *Nature* **450**, 89–92. doi:10.1038/NATURE06272

Boulanger Y, Gauthier S, Gray DR, Le Goff H, Lefort P, Morissette J (2013) Fire regime zonation under current and future climate over eastern Canada. *Ecological Applications* **23**, 904–923. doi:10.1890/12-0698.1

Carvalho A, Flannigan MD, Logan KA, Gowman LM, Miranda AI, Borrego C (2010) The impact of spatial resolution on area burned and fire occurrence projections in Portugal under climate change. *Climatic Change* **98**, 177–197. doi:10.1007/S10584-009-9667-2

Catry FX, Rego FC, Bacao F, Moreira F (2009) Modeling and mapping wildfire ignition risk in Portugal. *International Journal of Wildland Fire* **18**, 921–931. doi:10.1071/WF07123

Chang Y, Zhu ZL, Bu RC, Chen HW, Feng YT, Li YH, Hu YM, Wang ZC (2013) Predicting fire occurrence patterns with logistic regression in Heilongjiang Province, China. *Landscape Ecology* **28**, 1989–2004. doi:10.1007/S10980-013-9935-4

Chang Y, Zhu ZL, Bu RC, Li YH, Hu YM (2015) Environmental controls on the characteristics of mean number of forest fires and mean forest area burned (1987–2007) in China. *Forest Ecology and Management* **356**, 13–21. doi:10.1016/J.FORECO.2015.07.012

Chen DM, Pereira JMC, Masiero A, Pirotti F (2017) Mapping fire regimes in China using MODIS active fire and burned area data. *Applied Geography* **85**, 14–26. doi:10.1016/J.APGEOG.2017.05.013

Chen YY, Yang K, He J, Qin J, Shi JC, Du JY, He Q (2011) Improving land surface temperature modeling for dry land of China. *Journal of Geophysical Research, D, Atmospheres* **116**, D20104. doi:10.1029/2011JD015921

Dai YF, Yao TD, Li XY, Ping F (2018) The impact of lake effects on the temporal and spatial distribution of precipitation in the Nam Co basin, Tibetan Plateau. *Quaternary International* **475**, 63–69. doi:10.1016/J.QUAINT.2016.01.075

De'ath G (2007) Boosted trees for ecological modeling and prediction. *Ecology* **88**, 243–251. doi:10.1890/0012-9658(2007)88[243:BTFEMA]2.0.CO;2

Dreessen J, Sullivan J, Delgado R (2016) Observations and impacts of transported Canadian wildfire smoke on ozone and aerosol air quality in the Maryland region on June 9–12, 2015. *Journal of the Air & Waste Management Association* **66**, 842–862. doi:10.1080/10962247.2016.1161674

Elith J, Leathwick JR, Hastie T (2008) A working guide to boosted regression trees. *Journal of Animal Ecology* **77**, 802–813. doi:10.1111/J.1365-2656.2008.01390.X

Evans JS, Ram Karthik (2018) spatialEco. *R* package version 0.1.1–1. Available at R Core Team https://CRAN.R-project.org/package=spatialEco [Verified 20 June 2019]

Flannigan MD, Logan KA, Amiro BD, Skinner WR, Stocks BJ (2005) Future area burned in Canada. *Climatic Change* **72**, 1–16. doi:10.1007/S10584-005-5935-Y

Flannigan MD, Krawchuk MA, de Groot WJ, Wotton BM, Gowman LM (2009) Implications of changing climate for global wildland fire. *International Journal of Wildland Fire* **18**, 483–507. doi:10.1071/WF08187

Fox J, Monette G (1992) Generalized collinearity diagnostics. *Journal of the American Statistical Association* **87**, 178–183. doi:10.1080/01621459.1992.10475190

Friedman JH (2001) Greedy function approximation: a gradient boosting machine. *Annals of Statistics* **29**, 1189–1232. doi:10.1214/AOS/1013203451

Ganteaume A, Camia A, Jappiot M, San Miguel-Ayanz J, Long-Fournel M, Lampin C (2013) A review of the main driving factors of forest fire ignition over Europe. *Environmental Management* **51**, 651–662. doi:10.1007/S00267-012-9961-Z

Giglio L, Boschetti L, Roy DP, Humber ML, Justice CO (2018) The Collection 6 MODIS burned area mapping algorithm and product. *Remote Sensing of Environment* **217**, 72–85. doi:10.1016/J.RSE.2018.08.005

Greenwell B, Boehmke B, Cunningham J, Developers GBM (2018) gbm: Generalized Boosted Regression Models. *R* package version 2.1.4. Available at R Core Team https://CRAN.R-project.org/package=gbm [Verified 16 June 2018]

Guo FT, Zhang LJ, Jin S, Tigabu M, Su ZW, Wang WH (2016) Modeling anthropogenic fire occurrence in the boreal forest of China using logistic regression and random forests. *Forests* **7**, 250. doi:10.3390/F7110250

Guo FT, Su ZW, Wang GY, Sun L, Tigabu M, Yang XJ, Hu HQ (2017) Understanding fire drivers and relative impacts in different Chinese forest ecosystems. *The Science of the Total Environment* **605**, **606**, 411–425. doi:10.1016/J.SCITOTENV.2017.06.219

Hawbaker TJ, Radeloff VC, Stewart SI, Hammer RB, Keuler NS, Clayton MK (2013) Human and biophysical influences on fire occurrence in the United States. *Ecological Applications* **23**, 565–582. doi:10.1890/12-1816.1

Hijmans RJ, Cameron SE, Parra JL, Jones PG, Jarvis A (2005) Very-high-resolution interpolated climate surfaces for global land areas. *International Journal of Climatology* **25**, 1965–1978. doi:10.1002/JOC.1276

Huang Y, Salama MS, Su ZB, van der Velde R, Zheng DH, Krol MS, Hoekstra AY, Zhou YX (2016) Effects of roughness length parameterizations on regional-scale land surface modeling of alpine grasslands in

the Yangtze River Basin. *Journal of Hydrometeorology* **17**, 1069–1085. doi:10.1175/JHM-D-15-0049.1

Keane RE, Mahalovich MF, Bollenbacher BL, Manning ME, Loehman RA, Jain TB, Holsinger LM, Larson AJ (2018) Effects of climate change on forest vegetation in the Northern Rockies. In 'Climate change and Rocky Mountain ecosystems'. (Eds JE Halofsky, DL Peterson) pp. 59–95. (Springer International Publishing: Cham, Switzerland).

Li SF, Hughes AC, Su T, Anberree JL, Oskolski AA, Sun M, Ferguson DK, Zhou ZK (2017) Fire dynamics under monsoonal climate in Yunnan, SW China: past, present and future. *Palaeogeography, Palaeoclimatology, Palaeoecology* **465**, 168–176. doi:10.1016/J.PALAEO.2016.10.028

Liu YQ, Goodrick SL, Stanturf JA (2013) Future US wildfire potential trends projected using a dynamically downscaled climate change scenario. *Forest Ecology and Management* **294**, 120–135. doi:10.1016/J.FORECO.2012.06.049

Liu ZH, Wimberly MC (2015) Climatic and landscape influences on fire regimes from 1984 to 2010 in the western United States. *PLoS One* **10**, e0140839. doi:10.1371/JOURNAL.PONE.0140839

Liu ZH, Wimberly MC (2016) Direct and indirect effects of climate change on projected future fire regimes in the western United States. *The Science of the Total Environment* **542**, 65–75. doi:10.1016/J.SCITOTENV.2015.10.093

Liu ZH, Yang J (2014) Quantifying ecological drivers of ecosystem productivity of the early-successional boreal *Larix gmelinii* forest. *Ecosphere* **5**, 84. doi:10.1890/ES13-00372.1

Liu ZH, Yang J, Chang Y, Weisberg PJ, He HS (2012) Spatial patterns and drivers of fire occurrence and its future trend under climate change in a boreal forest of north-east China. *Global Change Biology* **18**, 2041–2056. doi:10.1111/J.1365-2486.2012.02649.X

Malevsky-Malevich SP, Molkentin EK, Nadyozhina ED, Shklyarevich OB (2008) An assessment of potential change in wildfire activity in the Russian boreal forest zone induced by climate warming during the twenty-first century. *Climatic Change* **86**, 463–474. doi:10.1007/S10584-007-9295-7

Meinshausen M, Smith SJ, Calvin K, Daniel JS, Kainuma MLT, Lamarque JF, Matsumoto K, Montzka SA, Raper SCB, Riahi K, Thomson A, Velders GJM, van Vuuren DPP (2011) The RCP greenhouse gas concentrations and their extensions from 1765 to 2300. *Climatic Change* **109**, 213–241. doi:10.1007/S10584-011-0156-Z

Mitchell RJ, Liu YQ, O'Brien JJ, Elliott KJ, Starr G, Miniat CF, Hiers JK (2014) Future climate and fire interactions in the south-eastern region of the United States. *Forest Ecology and Management* **327**, 316–326. doi:10.1016/J.FORECO.2013.12.003

Nitschke CR, Innes JL (2008) Climatic change and fire potential in south-central British Columbia, Canada. *Global Change Biology* **14**, 841–855. doi:10.1111/J.1365-2486.2007.01517.X

O'Donnell AJ, Boer MM, McCaw WL, Grierson PF (2011) Climatic anomalies drive wildfire occurrence and extent in semi-arid shrublands and woodlands of south-west Australia. *Ecosphere* **2**, 127. doi:10.1890/ES11-00189.1

Pan G, Pan D, Zhang HP (2013) Effects of forest fire on mixed forest of *Pinus massoniana* and *Cunninghamia lanceolata. Guangxi Forestry Science* **42**, 333–338. [in Chinese with English abstract]

Parisien MA, Moritz MA (2009) Environmental controls on the distribution of wildfire at multiple spatial scales. *Ecological Monographs* **79**, 127–154. doi:10.1890/07-1289.1

Parks SA, Parisien MA, Miller C (2011) Multiscale evaluation of the environmental controls on burn probability in a southern Sierra Nevada landscape. *International Journal of Wildland Fire* **20**, 815–828. doi:10.1071/WF10051

Pausas JG, Bradstock RA (2007) Fire persistence traits of plants along a productivity and disturbance gradient in mediterranean shrublands of south-east Australia. *Global Ecology and Biogeography* **16**, 330–340. doi:10.1111/J.1466-8238.2006.00283.X

Peduzzi P, Concato J, Kemper E, Holford TR, Feinstein AR (1996) A simulation study of the number of events per variable in logistic regression analysis. *Journal of Clinical Epidemiology* **49**, 1373–1379. doi:10.1016/S0895-4356(96)00236-3

Piao SL, Fang JY, Ji W, Guo QH, Ke JH, Tao S (2004) Variation in a satellite-based vegetation index in relation to climate in China. *Journal of Vegetation Science* **15**, 219–226. doi:10.1658/1100-9233(2004)015[0219:VIASVI]2.0.CO;2

Pitman AJ, Narisma GT, McAneney J (2007) The impact of climate change on the risk of forest and grassland fires in Australia. *Climatic Change* **84**, 383–401. doi:10.1007/S10584-007-9243-6

Preisler HK, Brillinger DR, Burgan RE, Benoit JW (2004) Probability-based models for estimation of wildfire risk. *International Journal of Wildland Fire* **13**, 133–142. doi:10.1071/WF02061

R Core Team (2017) R: A language and environment for statistical computing. R Foundation for Statistical Computing. (Vienna, Austria) Available at https://www.R-project.org [Verified 4 November 2019]

Romero-Ruiz M, Etter A, Sarmiento A, Tansey K (2010) Spatial and temporal variability of fires in relation to ecosystems, land tenure and rainfall in savannas of northern South America. *Global Change Biology* **16**, 2013–2023. doi:10.1111/J.1365-2486.2009.02081.X

Russell-Smith J, Yates CP, Whitehead PJ, Smith R, Craig R, Allan GE, Thackway R, Frakes I, Cridland S, Meyer MCP, Gill M (2007) Bushfires 'Down Under': patterns and implications of contemporary Australian landscape burning. *International Journal of Wildland Fire* **16**, 361–377. doi:10.1071/WF07018

Shirazi Z, Guo HD, Chen F, Yu B, Li B (2017) Assessing the impact of climatic parameters and their inter-annual seasonal variability on fire activity using time series satellite products in south China (2001–2014). *Natural Hazards* **85**, 1393–1416. doi:10.1007/S11069-016-2631-3

Sing T, Sander O, Beerenwinkel N, Lengauer T (2005) ROCR: visualizing classifier performance in R. *Bioinformatics* **21**, 3940–3941http://rocr.bioinf.mpi-sb.mpg.de. doi:10.1093/BIOINFORMATICS/BTI623

Stambaugh MC, Guyette RP (2008) Predicting spatiotemporal variability in fire return intervals using a topographic roughness index. *Forest Ecology and Management* **254**, 463–473. doi:10.1016/J.FORECO.2007.08.029

Syphard AD, Radeloff VC, Keeley JE, Hawbaker TJ, Clayton MK, Stewart SI, Hammer RB (2007) Human influence on California fire regimes. *Ecological Applications* **17**, 1388–1402. doi:10.1890/06-1128.1

Tian XR, Zhao FJ, Shu LF, Wang MY (2013) Distribution characteristics and the influence factors of forest fires in China. *Forest Ecology and Management* **310**, 460–467. doi:10.1016/J.FORECO.2013.08.025

van Lierop P, Lindquist E, Sathyapala S, Franceschini G (2015) Global forest area disturbance from fire, insect pests, diseases and severe weather events. *Forest Ecology and Management* **352**, 78–88. doi:10.1016/J.FORECO.2015.06.010

Vilar del Hoyo L, Isabel MPM, Vega FJM (2011) Logistic regression models for human-caused wildfire risk estimation: analysing the effect of the spatial accuracy in fire occurrence data. *European Journal of Forest Research* **130**, 983–996. doi:10.1007/S10342-011-0488-2

Wang MY, Shu LF, Tian XR, Zhao FJ (2010) Influences of ENSO events on forest fires in Heilong jiang province. *Forest Research* **23**, 644–648 [in Chinese with English abstract]

Westerling AL (2016) Increasing western US forest wildfire activity: sensitivity to changes in the timing of spring *Philosophical Transactions of the Royal Society B-Biological Sciences* **371**, 20150178.

Westerling AL, Hidalgo HG, Cayan DR, Swetnam TW (2006) Warming and earlier spring increase western US forest wildfire activity. *Science* **313**, 940–943. doi:10.1126/SCIENCE.1128834

Xu CH, Xu Y (2012) The projection of temperature and precipitation over China under RCP scenarios using a CMIP5 multi-model ensemble. *Atmospheric and Oceanic Science Letters* **5**, 527–533. doi:10.1080/16742834.2012.11447042

Yang G, Shu LF, Di XY (2012) Change trends of summer fire danger in Great Xing'an Mountains forest region of Heilongjiang Province, northeast China under climate change. *Ying Yong Sheng Tai Xue Bao* **23**, 3157–3163 [in Chinese with English abstract]

Yang YK, Xiao PF, Feng XZ, Li HX (2017) Accuracy assessment of seven global land cover datasets over China. *ISPRS Journal of Photogrammetry and Remote Sensing* **125**, 156–173. doi:10.1016/J.ISPRSJPRS.2017.01.016

Zhang Y, Lim S (2019) Drivers of wildfire occurrence patterns in the inland riverine environment of New South Wales, Australia. *Forests* **10**, 524. doi:10.3390/F10060524

Zhang ZQ, Zhong JJ, Lv XG, Tong SZ, Wang GP (2015) Climate, vegetation, and human influences on late-Holocene fire regimes in the Sanjiang plain, north-eastern China. *Palaeogeography, Palaeoclimatology, Palaeoecology* **438**, 1–8. doi:10.1016/J.PALAEO.2015.07.028

Zhao FJ, Shu LF, Tian XR, Wang MY (2009) Change trends of forest fire danger in Yunnan Province in 1957–2007. *Shengtaixue Zazhi* **28**, 2333–2338. [in Chinese with English abstract]

Zumbrunnen T, Bugmann H, Conedera M, Burgi M (2009) Linking forest fire regimes and climate – a historical analysis in a dry inner Alpine valley. *Ecosystems* **12**, 73–86. doi:10.1007/S10021-008-9207-3